

Biocompatible diimidazolium based ionic liquid system for enhancing the solubility of paclitaxel

Yanhui Hu,^{a,b,c} Hua Yue,^{b,c} Shiqi Huang,^b Bingxi Song,^{b,c} Yuyuan Xing,^{b,c} Minmin Liu,^b Gongying Wang,^{*a,c} Yanyan Diao^{*b,d,e}, Suojiang Zhang^{*b,d}

a Chengdu Institute of Organic Chemistry, Chinese Academy of Sciences, Chengdu 610041, China

b Beijing Key Laboratory of Ionic Liquids Clean Process, State Key Laboratory of Biochemical Engineering, Institute of Process Engineering, Chinese Academy of Sciences, Beijing, 100190, China

c University of Chinese Academy of Sciences, Beijing, 100049, China

d Longzihu New Energy Laboratory, Zhengzhou Institute of Emerging Industrial Technology, Henan University, Zhengzhou 450000, P. R. China

e School of Chemical & Environmental Engineering, China University of Mining and Technology (Beijing), Beijing 100083, P. R. China

*Corresponding Author: Gongying Wang, Yanyan Diao, Suojiang Zhang

Tel/Fax: 86-10-82544875, E-mail: wanggongying1102@126.com, yydiao@ipe.ac.cn, sjzhang@ipe.ac.cn

Characterizations of ILs

NMR as shown in Figure S1-S12, were carried out to identify the structures of the prepared diimidazole ILs.

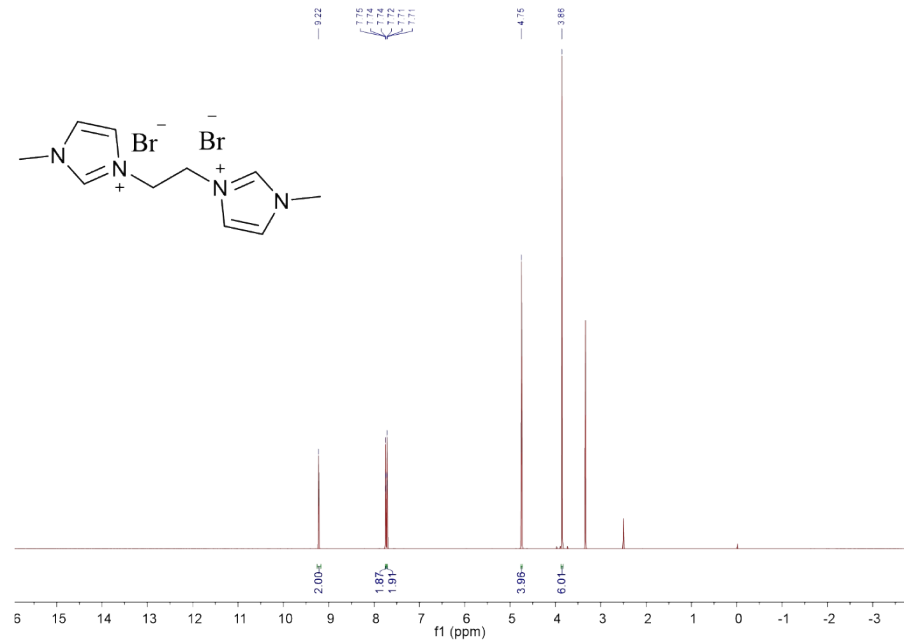


Fig. S1 The ¹H NMR spectrum of [C₂(MIM)₂][Br]₂ (DMSO)

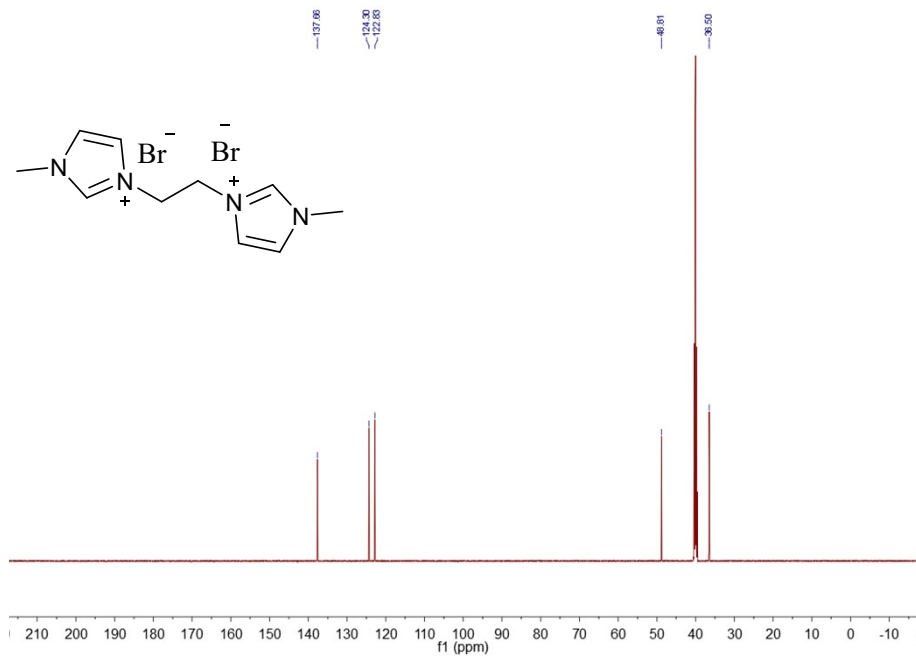


Fig. S2 The ^{13}C NMR spectrum of $[\text{C}_2(\text{MIM})_2][\text{Br}]_2$ (DMSO)

$[\text{C}_2(\text{MIM})_2][\text{Br}]_2$: ^1H NMR (600 MHz, DMSO) δ 9.22 (s, 2H), 7.74 (t, J = 1.7 Hz, 2H), 7.71 (t, J = 1.7 Hz, 2H), 4.75 (s, 4H), 3.86 (s, 6H). ^{13}C NMR (151 MHz, DMSO) δ 137.66, 124.30, 122.83, 48.81, 36.50.

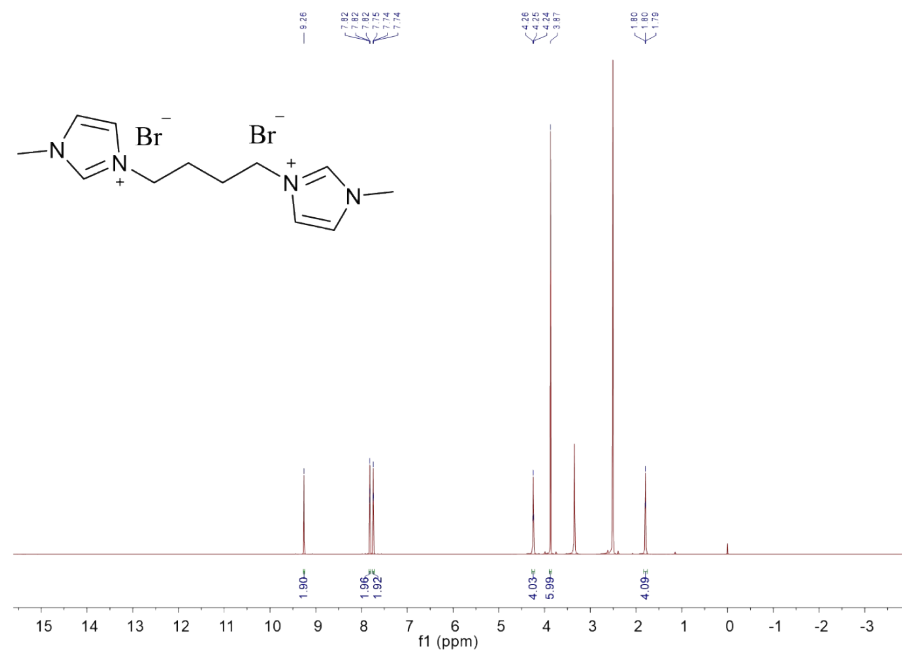


Fig. S3 The ^1H NMR spectrum of $[\text{C}_4(\text{MIM})_2][\text{Br}]_2$ (DMSO)

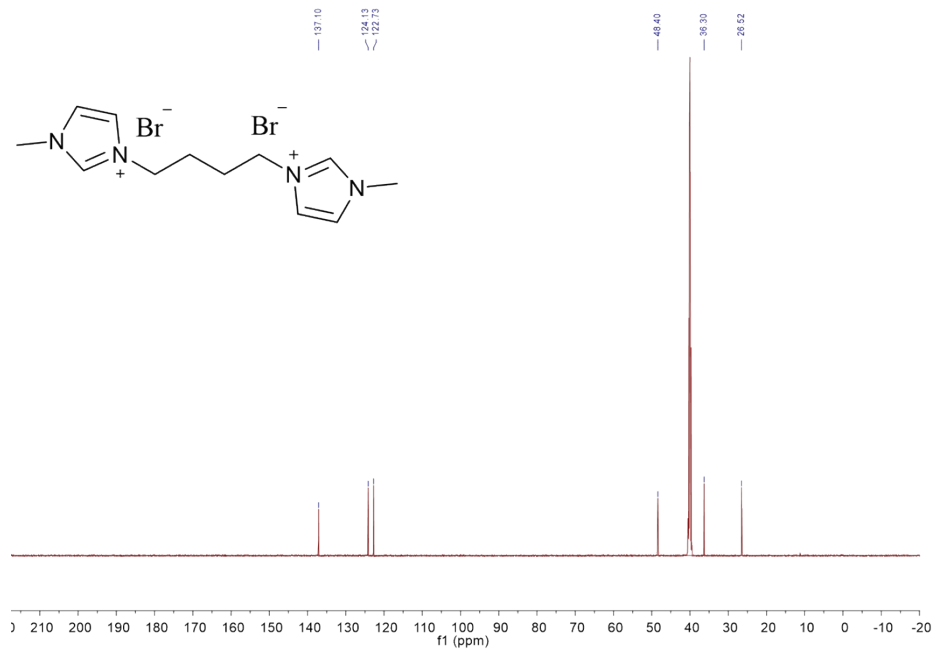


Fig. S4 The ^{13}C NMR spectrum of $[C_4(MIM)_2][Br]_2$ (DMSO)

$[C_4(MIM)_2][Br]_2$: 1H NMR (600 MHz, DMSO) δ 9.26 (s, 2H), 7.82 (t, J = 1.7 Hz, 2H), 7.74 (t, J = 1.5 Hz, 2H), 4.25 (t, J = 5.7 Hz, 4H), 3.87 (s, 6H), 1.80 (t, J = 2.8 Hz, 4H). ^{13}C NMR (151 MHz, DMSO) δ 137.00, 124.13, 122.73, 48.40, 36.30, 26.52.

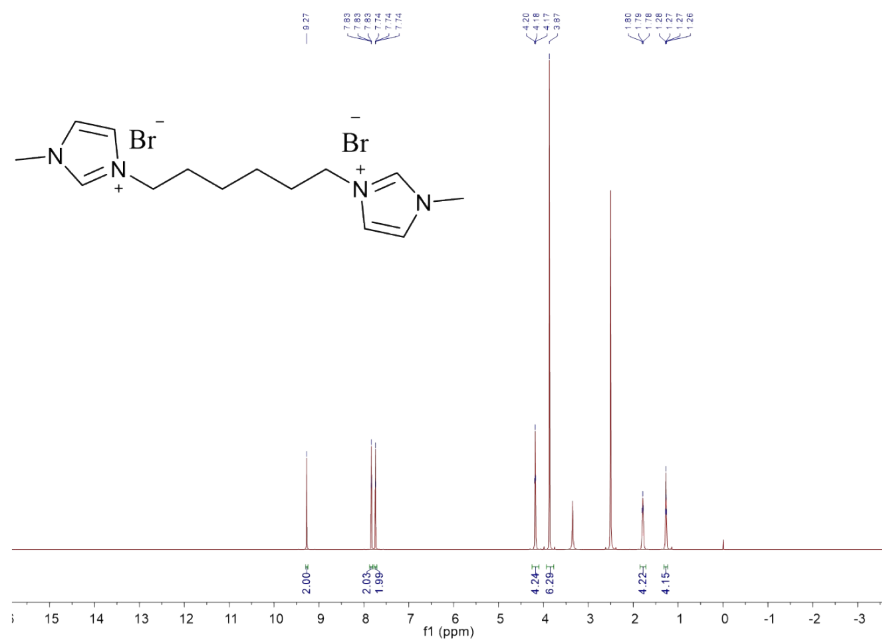


Fig. S5 The 1H NMR spectrum of $[C_6(MIM)_2][Br]_2$ (DMSO)

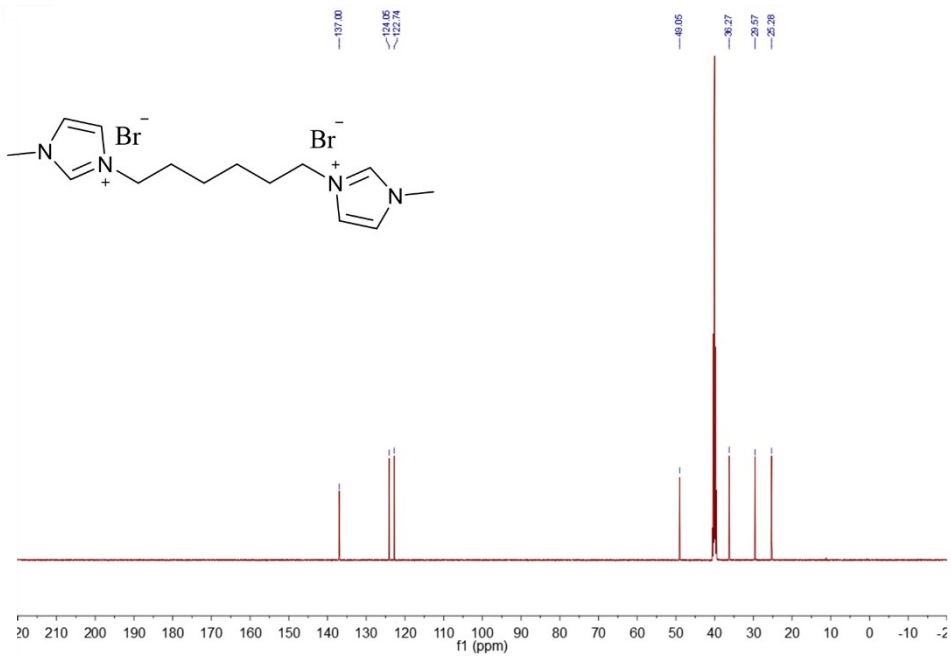


Fig. S6 The ^{13}C NMR spectrum of $[\text{C}_6(\text{MIM})_2]\text{[Br]}_2$ (DMSO)

$[\text{C}_6(\text{MIM})_2]\text{[Br]}_2$: ^1H NMR (600 MHz, DMSO) δ 9.27 (s, 2H), 7.83 (t, J = 1.6 Hz, 2H), 7.74 (t, J = 1.6 Hz, 2H), 4.18 (t, J = 7.2 Hz, 4H), 3.87 (s, 6H), 1.85-1.72 (m, 4H), 1.27 (dd, J = 8.7, 5.5 Hz, 4H). ^{13}C NMR (151 MHz, DMSO) δ 137.00, 124.05, 122.74, 49.05, 36.27, 29.57, 25.28.

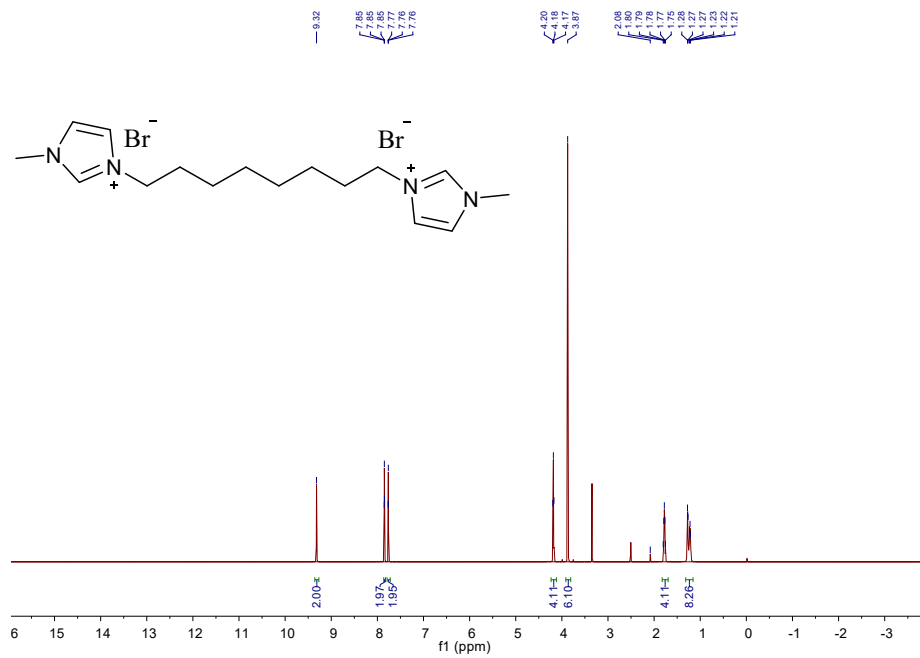


Fig. S7 The ^1H NMR spectrum of $[\text{C}_8(\text{MIM})_2]\text{[Br]}_2$ (DMSO)

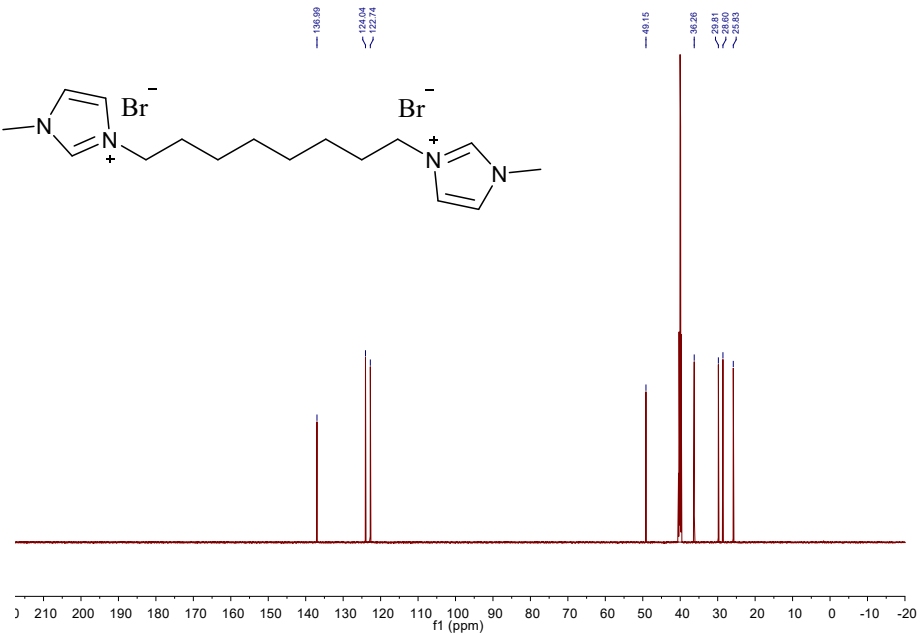


Fig. S8 The ^{13}C NMR spectrum of $[C_8(\text{MIM})_2][\text{Br}]_2$ (DMSO)

$[C_8(\text{MIM})_2][\text{Br}]_2$: ^1H NMR (600 MHz, DMSO) δ 9.32 (s, 2H), 7.85 (t, $J = 1.7$ Hz, 2H), 7.76 (t, $J = 1.7$ Hz, 2H), 4.18 (t, $J = 7.2$ Hz, 4H), 3.87 (s, 6H), 1.83-1.70 (m, 4H), 1.31-1.16 (m, 8H). ^{13}C NMR (151 MHz, DMSO) δ 136.99, 124.04, 122.74, 49.15, 36.26, 29.81, 28.60, 25.83.

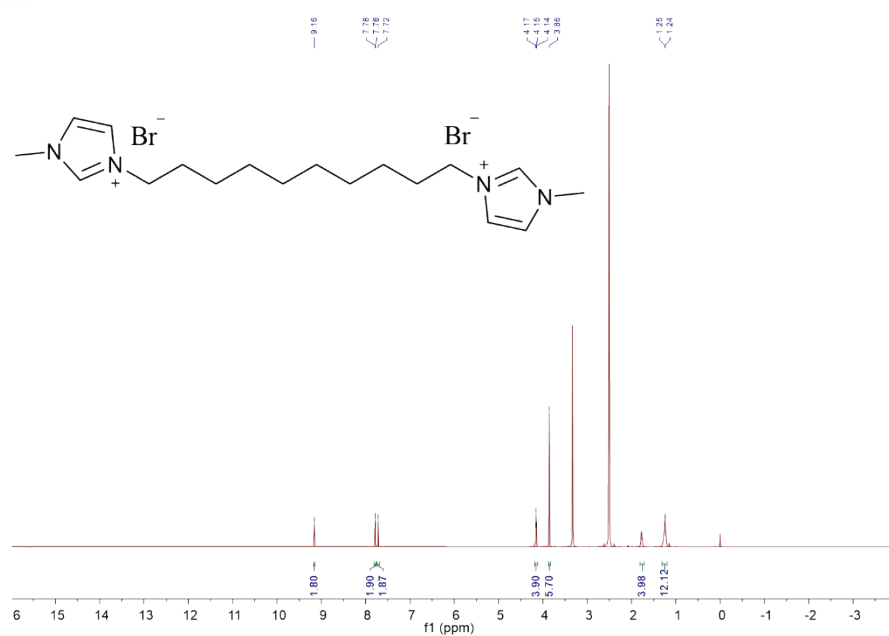


Fig. S9 The ^1H NMR spectrum of $[C_{10}(\text{MIM})_2][\text{Br}]_2$ (DMSO)

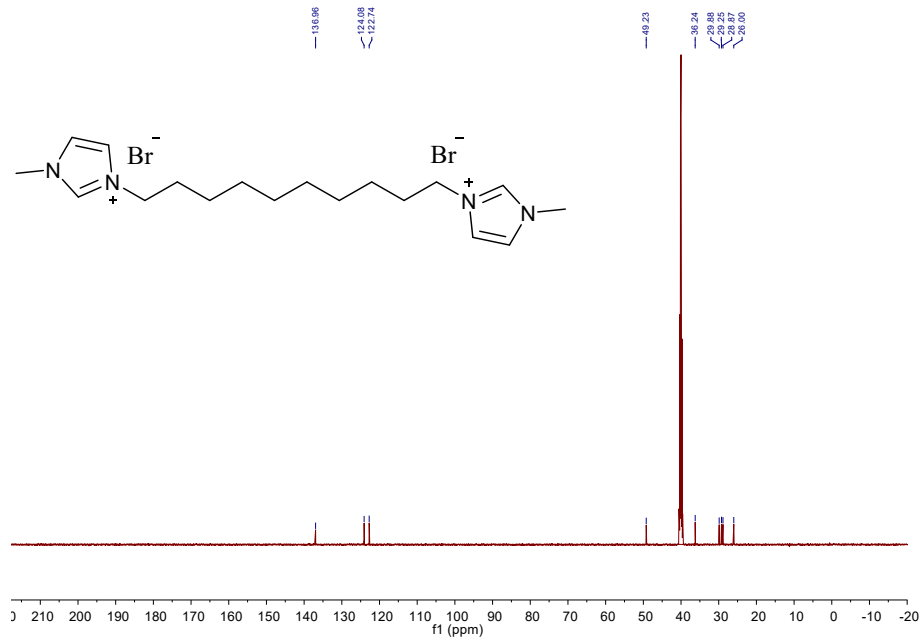


Fig. S10 The ^{13}C NMR spectrum of $[C_{10}(\text{MIM})_2][\text{Br}]_2$ (DMSO)

$[C_{10}(\text{MIM})_2][\text{Br}]_2$: ^1H NMR (600 MHz, DMSO) δ 9.16 (s, 2H), 7.78 (d, J = 1.6 Hz, 2H), 7.72 (s, 2H), 4.15 (t, J = 7.2 Hz, 4H), 3.86 (s, 6H), 1.81-1.72 (m, 4H), 1.25 (d, J = 4.0 Hz, 12H). ^{13}C NMR (151 MHz, DMSO) δ 136.96, 124.08, 122.74, 49.23, 36.24, 29.88, 29.25, 28.87, 26.00.

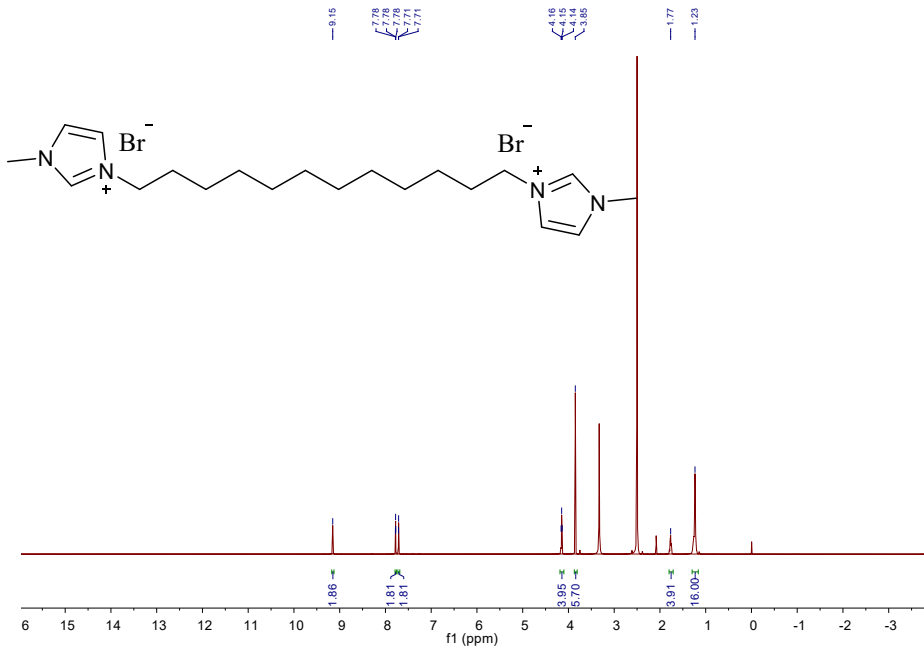


Fig. S11 The ^1H NMR spectrum of $[C_{12}(\text{MIM})_2][\text{Br}]_2$ (DMSO)

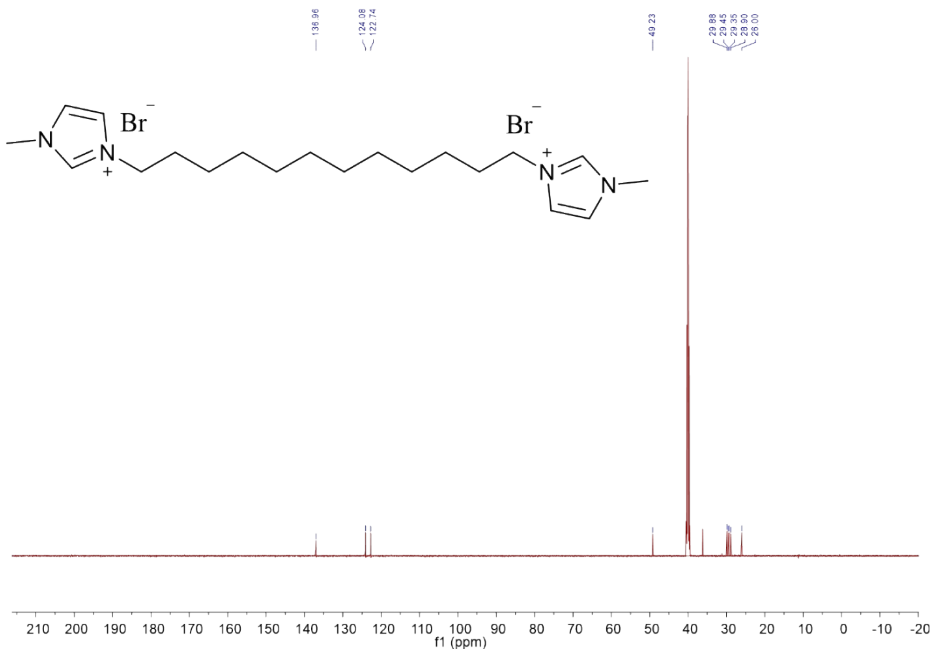
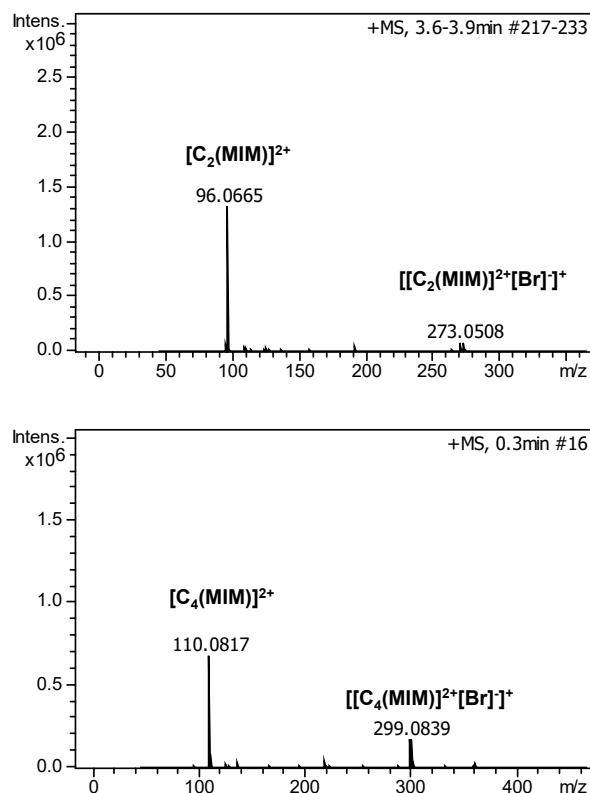


Fig. S12 The ^{13}C NMR spectrum of $[\text{C}_{12}(\text{MIM})_2]^{\text{2}+}[\text{Br}]_2$ (DMSO)

$[\text{C}_{12}(\text{MIM})_2]^{\text{2}+}[\text{Br}]_2$: ^1H NMR (600 MHz, DMSO) δ 9.15 (s, 2H), 7.78 (t, J = 1.6 Hz, 2H), 7.71 (d, J = 1.6 Hz, 2H), 4.15 (t, J = 7.2 Hz, 4H), 3.85 (s, 6H), 1.77 (s, 4H), 1.23 (s, 16H). ^{13}C NMR (151 MHz, DMSO) δ 136.96, 124.08, 122.74, 49.23, 29.88, 29.40, 28.90, 26.00.



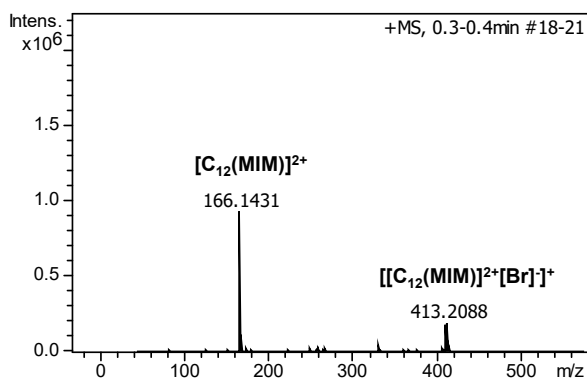
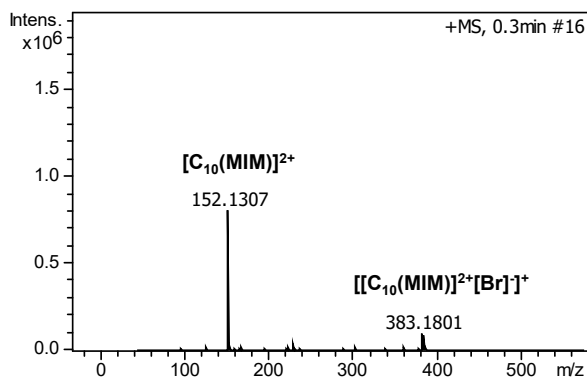
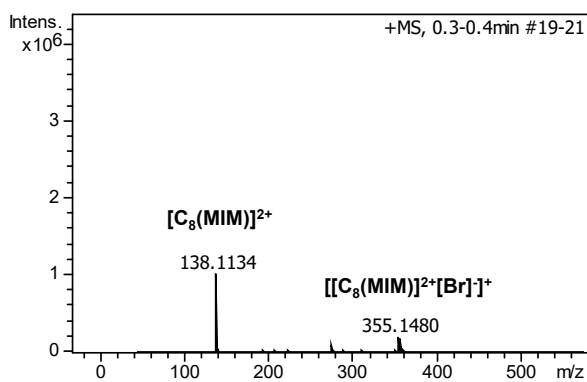
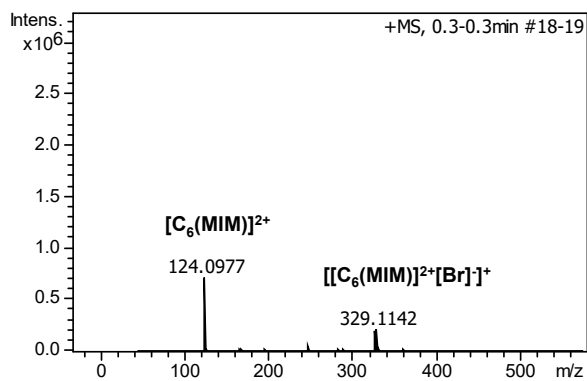


Fig. S13 ESI-MS spectrums of diimidazolium based ILs.

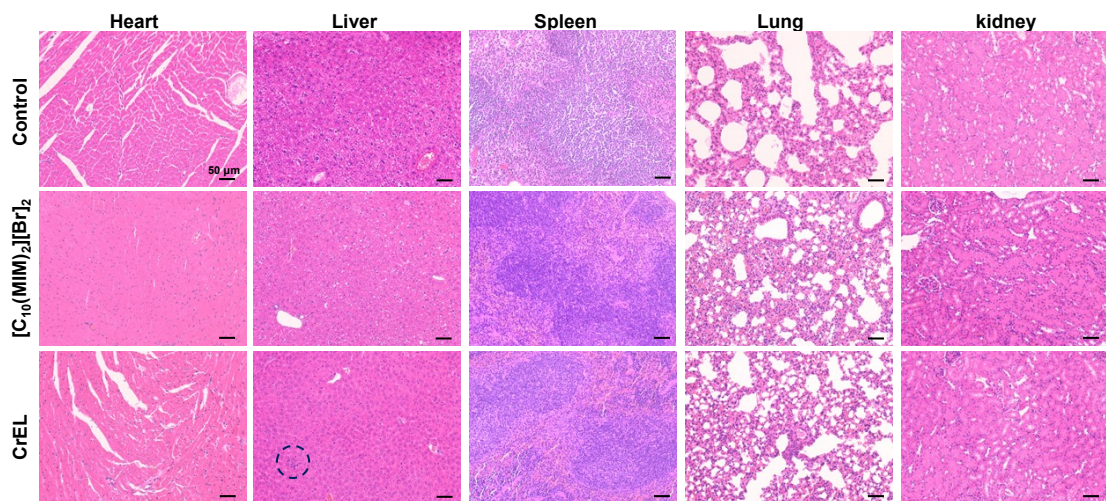


Fig. S14 Representative H&E staining of heart, liver, spleen, lung, and kidney tissues for mice by oral administration after day 7 with the dose of 250 $\mu\text{mol}/\text{kg}$ $[C_{10}(MIM)_2][Br]_2$ or CrEL. The dashed area represents inflammatory infiltration.

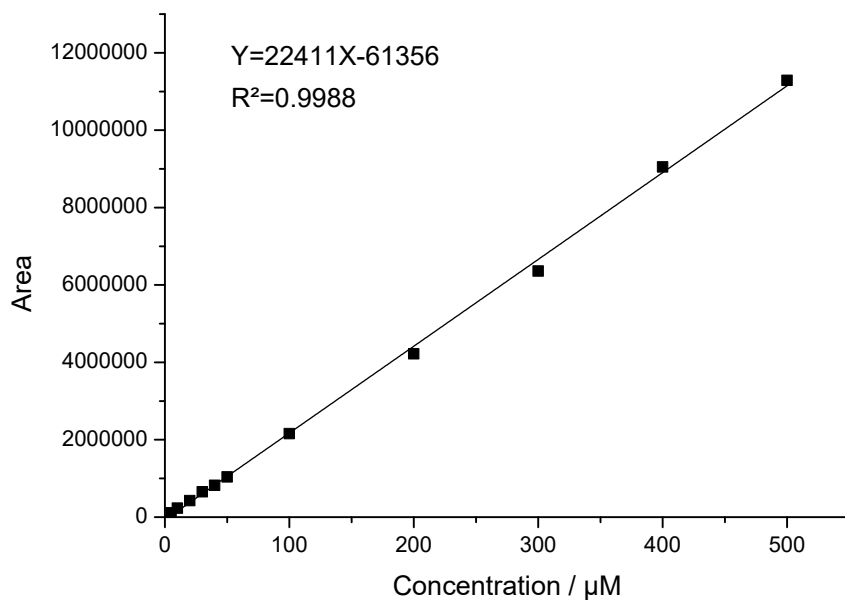


Fig. S15 The standard curve of peak area and PTX concentration conversion (5-500 μM) by UPLC at 227 nm.

Table S1 The comparation of cationic logP between mono-imidazole and diimidazole ILs predicted by Marvinsketch

Carbon number of cationic alkyl chain	Cationic logP of mono-imidazolium based ILs	Cationic logP of diimidazolium based ILs
2	-2.48	-5.85
4	-1.52	-5.27

6	0.39	-4.38
8	1.28	-3.49
10	2.17	-2.61
12	3.06	-1.72
